Nanoscale

RSC Publishing

COMMUNICATION

View Article Online
View Journal | View Issue

Edge-tailored graphene oxide nanosheet-based field effect transistors for fast and reversible electronic detection of sulfur dioxide†

Cite this: *Nanoscale*, 2013, **5**, 537

Received 14th September 2012
Accepted 24th November 2012

DOI: 10.1039/c2nr32752j

www.rsc.org/nanoscale

Fangping Shen,‡[abc] Dong Wang,‡[a] Rui Liu,[a] Xianfeng Pei,[a] Ting Zhang*[a] and Jian Jin*[a]

Graphene oxide was tailored into GO nanosheets with periodic acid treatment. Interestingly, the latter have a superior sensing performance for the fast and reversible detection of SO_2 compared with the former at room temperature. Its sensing mechanism was proposed from the structural changes of the GO nanosheets during the sensing and recovering processes.

Sulfur dioxide (SO_2) has been regarded as one of the six common air pollutants (the other pollutants are ozone, particulate matter, nitrogen dioxide, carbon monoxide, and lead). Exposure to these pollutants is associated with numerous effects on human health and the environment, and they may cause property damage. High concentrations of SO_2 generally lead to the formation of other gaseous sulfur oxides (SO_x), which react with other compounds in the atmosphere to form small particles. These particles penetrate deeply into the sensitive parts of the lungs and can cause or worsen respiratory disease, and can aggravate existing heart disease.[1,2] Therefore, convenient SO_2 sensors that allow for rapid and accurate detection, with a high sensitivity and selectivity, are crucial for providing adequate health and environmental protection. Electrochemistry, fluorimetry, gas chromatography, and the modified Rankine method are currently used for SO_2 detection. However, these techniques are limited to the use of bulky and expensive equipment and time-consuming detection processes, which require high power-consumption and/or high temperature.[3] The present study has been focused on developing new generations of miniature, low-power, and portable nanoelectronic sensors.

Chemiresistive sensors based on nanostructured materials with an extremely high surface area offer significant advantages over conventional metal oxide-based chemiresistors, in terms of a quick response, easy operation, and high sensitivity.[4–12] Even so, detection of SO_2 remains a challenge because SO_2 is prone to irreversibly react with active groups. A prolonged UV irradiation and heating process are commonly needed to reverse the signal. For example, a graphene based SO_2 field effect transistor (FET) is required to anneal at 100 °C in a high vacuum in order to achieve complete recovery of the sensor.[13] Semiconducting metal oxide sensors are necessarily operated at high temperatures (200–450 °C) in order to enhance the desorption rate and chemical reactivity between the SO_2 and the metal oxide.[14] Recently, graphene oxide (GO) and reduced GO have been demonstrated as highly sensitive chemical and biological sensors.[15–20] GO is suitable for electronic sensing applications due to its versatile properties, such as ease of processing, rich oxygen-containing functional groups, and high solubility in various solvents. Its electrical properties can be tuned *via* chemical functionalization to improve the sensitivity and selectivity, and solution based processes can simplify the integration of GO/rGO sheets into planar thin-film based sensors by ink-jet printing or just drop-deposition methods.

We demonstrate herein a GO nanosheet-based FET which does not require heat or photo-irradiation for fast, quantitative, and reversible SO_2 detection. The FET, made of chemically edge-tailored GO nanosheets can selectively detect SO_2 gas at room temperature in ambient air, which provides a potential for the development of GO-based miniaturized, portable, *in situ* sensors. We recently reported a unique chemical way to cut GO into a nanometer scale and simultaneously tailor its edge into a continuous and linear array of quinoid structures, which offered it a special ability to coordinate with some species, such as H^+ and various metal ions. The extremely sensitive pH-dependent property of the edge-tailored GO nanosheets inspired us to investigate their potential to be used as an acidic gas sensor. Our results demonstrate that the edge-tailored GO nanosheet-based FET shows a fast and reversible response to SO_2 gas with perfect sensitivity and selectivity.

Edge-tailored GO nanosheets were made by chemical exfoliation of natural graphite powders using a modified Hummers' method at first, and then further oxidized by a periodic acid. The variation of the lateral size of the GO before and after periodic acid treatment is

[a]*i-Lab, Suzhou Institute of Nano-tech and Nano-bionics, Chinese Academy of Sciences, Suzhou, 215123, China. E-mail: jjin2009@sinano.ac.cn; tzhang2009@sinano.ac.cn*
[b]*Institute of Biophysics, Chinese Academy of Sciences, Beijing, 100101, China*
[c]*University of Chinese Academy of Sciences, Beijing, 100049, China*

† Electronic supplementary information (ESI) available. See DOI: 10.1039/c2nr32752j

‡ These authors contributed to this work equally.

shown in Fig. 1, as characterized by AFM measurements. The lateral size of the original GO treated only by Hummers' oxidation is relatively large and polydisperse (Fig. 1a). Its size distribution ranges widely from tens to more than two hundred nanometers. After treatment by periodic acid, the lateral size of the GO is decreased largely and becomes very uniform, with a size distribution of around 30 nm (Fig. 1b). Meanwhile, its edge is endowed with numerous quinoid groups in a linear array, which has been confirmed by fluorescence, FTIR, and XPS spectra (see ESI, Fig. S1–S4†). The thicknesses of the original GO and edge-tailored GO nanosheets are all less than 1.5 nm, as shown in their height profiles (the insets in Fig. 1a and b), which is consistent with that of the regular exfoliated GO sheets. AFM images of both the original and edge-tailored GO nanosheets indicate that the original GO was cut into nano-debris by a simple wet chemical method.

The GO-based FET devices were fabricated by drop-casting the dispersion of original GO and edge-tailored GO nanosheets onto gold interdigitated electrodes (Fig. 2a), on the top of SiO_2 as an insulating layer on a highly doped Si as the backgate, respectively. As shown in Fig. 2b, the GO nanosheets formed the thin film and bridged the interdigitated electrodes with a 5 μm gap. The *I–V* curve, monitored with a Keithley 2602 Source Meter at ambient conditions, is S-shaped, indicating weak conductivity (~a few nA) and high contact resistance due to the sheet-to-sheet junctions (Fig. 2c). The dynamic resistances ($R = dV/dI$ *versus* V) of the original GO and edge-tailored GO nanosheets are compared, as shown in Fig. S5.† It indicates a significant decrease in the conductance of the edge-tailored GO nanosheets. It is well known that GO can be considered as a two-dimensional network consisting of variable fractions of the sp^2 and sp^3 domains, and its electrical and chemical properties are highly determined by the oxygenated groups. While in our case a continuous and linear array of quinoid structures was formed on the edges during the synthesis of the GO nanosheets.[21] The GO nanosheets are highly hygroscopic so that the quinoid carbonyls adsorb water molecules in air and isomerize into phenolic hydroxyls. The participation of protons provides percolation pathways between the sp^2 domains, allowing a slight degree of conductivity to be restored. The real-time changes in the conductance of the GO nanosheets upon exposure to different relative humidity (RH) in air are reported in Fig. S6a.† It shows that the conductance increased with decreased RH. Backgated FET characteristics for the edge-tailored GO nanosheets devices were also collected. As shown in Fig. 2d, the devices exhibit typical p-type semiconducting behaviour in air, and the on/off ratios are generally between 10 and 100. This value is higher than that of most reported

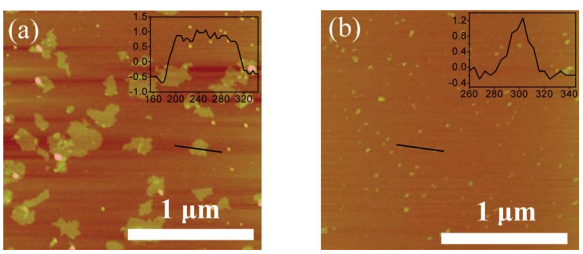

Fig. 1 2 μm × 2 μm AFM images of (a) the original GO and (b) edge-tailored GO nanosheets dropped on mica, and their height profiles are shown in the insets.

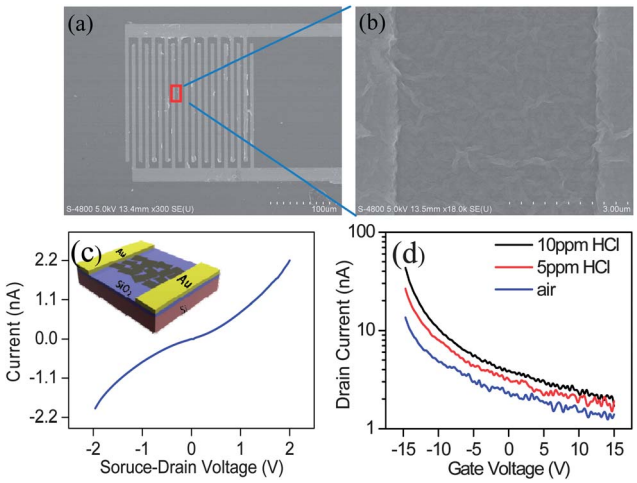

Fig. 2 SEM images of the interdigitated electrodes on the FET device (a) and the GO nanosheets bridging the two electrodes (b). (c) *I–V* curve of the edge-tailored GO nanosheet-based FET device at ambient conditions. The inset is the schematic representation of the backgated FET device where GO nanosheets integrate with each other to bridge a trench between the Cr/Au electrical contacts on a Si/SiO_2 substrate. (d) Source–drain current (I_{SD}) *versus* gate voltage (V_G) curves of the edge-tailored GO nanosheet-based FET device at 0, 5, and 10 ppm of HCl exposure, with a constant source–drain bias (V_{SD}) of 2 V.

graphene/rGO based FET devices (on/off ratios less than 10), which can be mainly attributed to the larger energy gap of the GO nanosheets, due to a stronger confinement effect, since they consist of finite numbers of atoms with smaller sp^2 domains.[22] The exposure of the device to 5 ppm and 10 ppm HCl vapor leads to an incremental positive shift of the I_{SD}–V_G characteristics and increases the conductance of the device. The sensing mechanism is depicted in Scheme 1, and shows that when the edge-tailored GO nanosheet-based devices are exposed to HCl vapour with a 65% relative humidity (RH), hydrochloric acid is formed on the nanosheets to produce protons (H^+), and then the extremely rich alpha-hydroxy-quinoid six-membered rings on the edges are first protonated by H^+, and then the protonated edges isomerize. This is equivalent to introducing holes into the valence band of the semiconducting GO nanosheets, thereby increasing the conductance. The protonation and isomerization processes are reversible so that the resistance of the device is totally recoverable. The photoluminescence is another piece of evidence to prove this mechanism (see ESI Fig. S3†). The edge-tailored GO nanosheets display an emission peak around 550 nm under acidic conditions at an excitation wavelength of 365 nm. It's the edge effect that enhances H^+ sensing, which indicates the potential application of GO nanosheet-based FET devices for SO_2 detection.

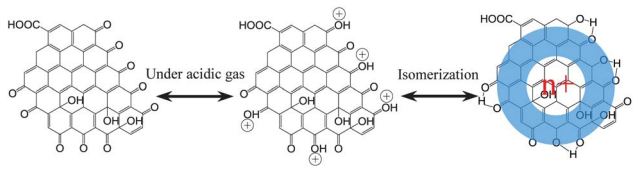

Scheme 1 Schematic of the sensing mechanism of the GO nanosheets under an acidic gas.

The electrical response of edge-tailored GO nanosheets to SO_2 was explored and compared with that of the original GO. The devices were tested under a constant source–drain bias of 0.8 V without gate voltage at room temperature with a 65% RH. SO_2 gas was pulsed onto the sensor surface using air with the same percentage of RH as the carrier gas. As shown in Fig. 3a, the edge-tailored GO nanosheet-based sensor device's exposure to different concentrations of SO_2 vapor result in a conductance increase, and the response of the device enhances with the increase of SO_2 concentration. The detection range of this specific test ranges from 5 ppm to 1100 ppm. The original GO based devices, however, show a much smaller response to SO_2 (Fig. 3b) and have a much slower response and recovery time. Unlike most recent reported rGO/graphene based electronic gas sensors,[23,24] our devices show a remarkably fast response time and are totally reversible. The response time is within a few seconds and the recovery time is within a few minutes at room temperature (Fig. S6b†). Generally for rGO/graphene based electronic gas sensors, their thermal energy at room temperature is not high enough to overcome the activation energy needed for gas molecule desorption. For full recovery, UV exposure or a high temperature is required, which will increase the complexity and power consumption of the sensor device.[25–27] The fast response of our devices can be due to the hygroscopic nature of the GO nanosheets, which attract water molecules to the channel of the FET devices, and let SO_2 simultaneously react with water to form sulphurous acid to promote the fast protonation. The stability of the GO nanosheet-based sensors was also explored. 10 cycles of 500 ppm SO_2 vapor sensing is given in Fig. 3c which exhibits excellent reversibility. Five sensors were tested simultaneously under multiple cycles of 500 ppm SO_2, and the standard deviations of the sensitivity were calculated to be 0.12, 0.05, 0.04, 0.06 and 0.05, respectively (Fig. S7a†), which demonstrate the great precision of all the devices. The conductance baseline was measured continuously for 5 hours and compared with the baseline after 48 hours. The standard deviation of the baseline is calculated to be 1.2% over 2 days, which shows a great stability (Fig. S7b†). In a selective detection test, we further verified that the alpha-hydroxyquinoid six-membered ring of the GO nanosheets merely enhances the response to SO_2 and scarcely generates signal changes with other weak acidic gases or volatile organic compounds (VOCs). Fig. 3d shows that our devices exhibit no response when exposed to a series of 1000 ppm H_2S, 200 ppm ether (Et), 200 ppm ethyl acetate (EA), 200 ppm tetrahydrofuran (THF), 200 ppm formaldehyde (HCHO), and 200 ppm benzene (Benz). It should be mentioned here that the edge-tailored GO nanosheet-based FET devices responded to strong acidic gases, such as HCl and NO_2 (Fig. S8†). We found that the sensitivities to different acidic gases are correlated to the acid dissociation constant (K_a) (HCl:$K_a \approx 1$, Detection Limit (DL) = 1.5 ppm; H_2SO_3:$K_a = 1.54 \times 10^{-2}$, DL = 5 ppm; H_2S:$K_a = 9.1 \times 10^{-8}$, DL > 1000 ppm). For practical and accurate SO_2 sensing applications, chemical filters may be required to eliminate some of the interfering gases, and environmental factors, such as the O_2 concentration and level of RH must be well-controlled to get optimized sensor performance.

In conclusion, we demonstrated that the GO nanosheets derived from chemically tailoring the as-prepared GO act as a promising active material for SO_2 gas sensing. The edge-tailored GO nanosheet-based chemiresistive sensor readily achieved a wide range of sensitivity as well as a fast response and recovery time at room temperature. The sensing mechanism probably was ascribed to the holes induced as the edge-tailored GO nanosheets were protonated and isomerized when exposed to acidic gases. Moreover, the selectivity and precision were demonstrated, and the results revealed that the sensors posses a special selectivity for SO_2 gas.

This work is supported by the National Natural Science Foundation of China (Grant no. 91123034, 50973080, 21107132, 21004076) and the Science and Technology Program of Suzhou (SH201010, SYG201144). We thank the Platform of Characterization & Test and Nanofabrication of Suzhou Institute of Nanotech and Nanobionics, Chinese Academy of Sciences.

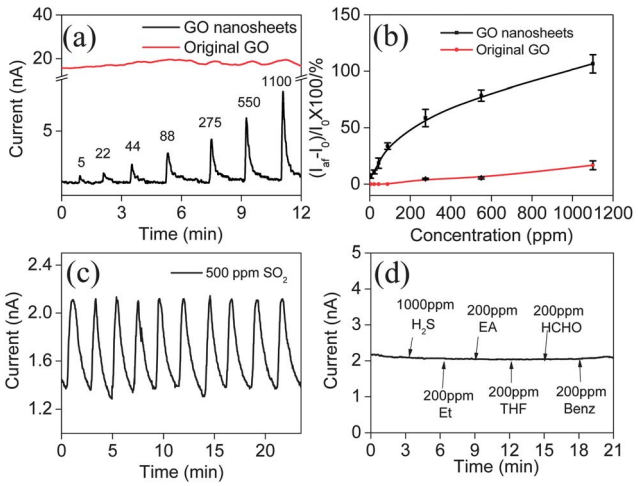

Fig. 3 Response of the original GO and edge-tailored GO nanosheet-based sensors to SO_2 gases. (a) Current *vs.* time curves for 5–1100 ppm of SO_2 for the original GO and edge-tailored GO nanosheets. (b) Sensitivities of the original GO and edge-tailored GO nanosheet-based sensors to SO_2 gas. (c) Ten cycles of precision test of the edge-tailored GO nanosheets for response to 500 ppm SO_2 gas. (d) Real time response of the edge-tailored GO nanosheets to H_2S, Et, EA, THF, HCHO, and Benz gases.

Notes and references

1 National Ambient Air Quality Standards (NAAQS) announced by US Environmental Protection Agency (EPA), 2010, June 22, http://www.epa.gov/air/criteria.html.
2 F. Sonni, F. Chinnici, N. Natali and C. Riponi, *Food Chem.*, 2011, **129**, 1193–1200.
3 A. W. E. Hodgson, P. Jacquinot and P. C. Hauser, *Anal. Chem.*, 1999, **71**, 2831–2837.
4 I. M. Feigel, H. Vedala and A. Star, *J. Mater. Chem.*, 2011, **21**, 8940–8954.
5 F. Schedin, A. K. Geim, S. V. Morozov, E. W. Hill, P. Blake, M. I. Katsnelson and K. S. Novoselov, *Nat. Mater.*, 2007, **6**, 652–655.
6 P. G. Collins, K. Bradley, M. Ishigami and A. Zettl, *Science*, 2000, **287**, 1801–1804.
7 T. H. Han, Y. K. Huang, A. T. Tan, V. P. Dravid and J. Huang, *J. Am. Chem. Soc.*, 2011, **133**, 15264–15267.

8 H. Vedala, D. C. Sorescu, G. P. Kotchey and A. Star, *Nano Lett.*, 2011, **11**, 2342–2347.
9 J. Kong, N. R. Franklin, C. W. Zhou, M. G. Chapline, S. Peng, K. J. Cho and H. J. Dai, *Science*, 2000, **287**, 622–625.
10 T. Zhang, S. Mubeen, N. V. Myung and M. A. Deshusses, *Nanotechnology*, 2008, **19**, 332001, 14pp.
11 T. Zhang, M. B. Nix, B. Y. Yoo, M. A. Deshusses and N. V. Myung, *Electroanalysis*, 2006, **18**, 1153–1158.
12 G. Lu, K. Yu, L. E. Ocola and J. Chen, *Chem. Commun.*, 2011, **47**, 7761–7763.
13 Y. Ren, C. Zhu, W. Cai, H. Li, H. Ji, I. Kholmanov, Y. Wu, R. D. Piner and R. S. Ruoff, *Appl. Phys. Lett.*, 2012, **100**, 163114.
14 E. Brunet, T. Maier, G. C. Mutinati, S. Steinhauer, A. Koeck, C. Gspan and W. Grogger, *Sens. Actuators, B*, 2012, **165**, 110–118.
15 Q. He, H. G. Sudibya, Z. Yin, S. Wu, H. Li, F. Boey, W. Huang, P. Chen and H. Zhang, *ACS Nano*, 2010, **4**, 3201–3208.
16 S. He, B. Song, D. Li, C. Zhu, W. Qi, Y. Wen, L. Wang, S. Song, H. Fang and C. Fan, *Adv. Funct. Mater.*, 2010, **20**, 453–459.
17 J. D. Fowler, M. J. Allen, V. C. Tung, Y. Yang, R. B. Kaner and B. H. Weiller, *ACS Nano*, 2009, **3**, 301–306.
18 Q. Mei and Z. Zhang, *Angew. Chem., Int. Ed.*, 2012, **51**, 5602–5606.
19 G. Lu, L. E. Ocola and J. Chen, *Appl. Phys. Lett.*, 2009, **94**, 083111.
20 G. Lu, L. E. Ocola and J. Chen, *Nanotechnology*, 2009, **20**, 445502.
21 D. Wang, L. Wang, X. Dong, Z. Shi and J. Jin, *Carbon*, 2012, **50**, 2147–2154.
22 F. Schwierz, *Nat. Nanotechnol.*, 2010, **5**, 487–496.
23 J. T. Robinson, F. K. Perkins, E. S. Snow, Z. Wei and P. E. Sheehan, *Nano Lett.*, 2008, **8**, 3137–3140.
24 F. Yavari and N. Koratkar, *J. Phys. Chem. Lett.*, 2012, **3**, 1746–1753.
25 Z. Chen, W. Ren, L. Gao, B. Liu, S. Pei and H.-M. Cheng, *Nat. Mater.*, 2011, **10**, 424–428.
26 J. D. Fowler, M. J. Allen, V. C. Tung, Y. Yang, R. B. Kaner and B. H. Weiller, *ACS Nano*, 2009, **3**, 301–306.
27 V. Dua, S. P. Surwade, S. Ammu, S. R. Agnihotra, S. Jain, K. E. Roberts, S. Park, R. S. Ruoff and S. K. Manohar, *Angew. Chem., Int. Ed.*, 2010, **49**, 2154–2157.

